

Demography of galactic technosignatures

Claudio Grimaldi,^{1*}

¹Laboratory of Physics of Complex Matter, Ecole Polytechnique Fédérale de Lausanne, Station 3, CP-1015 Lausanne, Switzerland

1 December 2020

ABSTRACT

Probabilistic arguments about the existence of technological life beyond Earth traditionally refer to the Drake equation to draw possible estimates of the number of technologically advanced civilizations releasing, either intentionally or not, electromagnetic emissions in the Milky Way. Here, we introduce other indicators than Drake’s number N_D to develop a demography of artificial emissions populating the Galaxy. We focus on three main categories of statistically independent signals (isotropic, narrow beams, and rotating beacons) to calculate the average number N_G of emission processes present in the Galaxy and the average number of them crossing Earth, \bar{k} , which is a quantity amenable to statistical estimation from direct observations. We show that \bar{k} coincides with N_D only for isotropic emissions, while \bar{k} can be orders of magnitude smaller than N_D in the case of highly directional signals. We further show that while N_D gives the number of emissions being released at the present time, N_G considers also the signals from no longer active emitters but whose emissions still occupy the Galaxy. We find that as long as the average longevity of the emissions is shorter than about 10^5 yr, N_G is fully determined by the rate of emissions alone, in contrast to N_D and \bar{k} which depend also on the emission longevity. Finally, using analytic formulas of N_G , N_D , and \bar{k} determined for each type of emission processes here considered, we provide a comprehensive overview of the values these quantities can possibly achieve as functions of the emission birthrates, longevities, and directionality.

Key words: Extraterrestrial intelligence – Astrobiology – Methods: statistical – Galaxy: disk

1 INTRODUCTION

As new extrasolar worlds are being routinely discovered, there is an ever mounting evidence that a significant fraction of exoplanets may have environmental conditions suitable for developing life (Dressing & Charbonneau 2013; Petigura et al. 2013; Zink & Hansen 2019). In the hunt for signs of life beyond the solar system, the search for biosignatures from the atmosphere and surface of extrasolar Earth-like planets is moving its first steps and will likely dominate the exoplanet science in the next decades (Kiang et al. 2018). The prospects of life elsewhere in the Galaxy have also reinvigorated the longstanding search for putative signs of technologically savvy life from beyond Earth. The search for such technosignatures is going indeed through a phase of intense activity, boosted primarily by large scale private initiatives such as the Breakthrough Listen program (Enriquez et al. 2017; Isaacson et al. 2017; Price et al. 2019) and benefiting of significant advances in detector technologies.

The searches for bio- and technosignatures are two complementary strategies in the general quest of finding life elsewhere as they probe different remotely detectable byproducts of life. Future searches for spectroscopic biosignatures will however target exoplanets up to only a few tens of light years from Earth (Seager 2018), while current telescopes are potentially capable of detecting, for example, radio emissions

from artificial sources of technological level comparable to our own located well beyond 100 ly from the Earth (Gray 2020). Moreover, searches for remotely detectable technosignatures probe a parameter search space so large that the absence of detection to date does not warrant any firm conclusion about the existence of potentially detectable exocivilizations (Wolfe et al. 1981; Tarter 2001). This point has been recently emphasized by Wright et al. (2018) who compare the tiny fraction of the parameter space explored so far to the ratio of the volume of a small swimming pool to that of the Earth’s oceans.

On the theoretical side, the prospects of technological life existing elsewhere and the probability of its detection are undetermined as well. In this context, the famous Drake equation has traditionally inspired the search for electromagnetic (EM) technosignatures (Drake 1961, 1965). In its compact form, the Drake equation equates the mean number of active emitters, N_D , with the product between the average rate of emergence of communicating civilizations, Γ , and the average longevity, \bar{L} , of the emission processes:

$$N_D = \Gamma \bar{L}. \quad (1)$$

In the original formulation of Eq. (1), Γ was expressed as a product of probability factors, later grouped in astrophysical and biological/evolutionary probability events (Prantzos 2013), though to be conducive to the emergence of technological life capable of releasing EM emissions. A vast literature has been devoted to the analysis of (1) (Ćirković 2004; Maccone 2010; Frank & Sullivan III 2016; Glade et al. 2016; Balbi

* E-mail: claudio.grimaldi@epfl.ch

2018) and to the discussion of each entry of the original Drake equation thought, nowadays, only the astrophysical contributions to Γ are known with some confidence (Anchordoqui et al. 2018; Prantzos 2019). Not surprisingly, lacking any empirical knowledge about the rate of abio- and technogenesis beyond Earth or the size of \bar{L} , estimates of N_D span several orders of magnitude, even for the Milky Way galaxy alone (Forgan 2009).

Although Eq. (1) is the most celebrated equation in the field of technosignatures, it is not the only vehicle to study their statistical properties. For example, of particular importance for assessing the probability of detection are the emission processes that cross our planet, as only those can be potentially detected (Grimaldi 2017). Their average number, denoted \bar{k} , is thus a quantity that can be empirically estimated from observations, at least in principle. In practice, however, the limited sensitivity of current telescopes and the aforementioned vastness of the parameter search space permits only a probabilistic inference of the range of possible values of \bar{k} compatible with observations (Grimaldi & Marcy 2018; Flodin 2019).

Even if \bar{k} is sometimes confused with the Drake number, it actually coincides with N_D only by assuming a constant birthrate of emissions that are either entirely isotropic, that is, radiating in all directions, or otherwise all directed towards our planet. In more general scenarios that contemplate anisotropic EM emissions, such as randomly directed beam-like signals or beacons sweeping across space, only the fraction of emissions directed towards the Earth can be potentially detected, implying $N_D \geq \bar{k}$.

Another quantity of interest discussed here is N_G , the average total number of emission processes present in the Galaxy. According to this definition, N_G contains both the processes generated by emitters that are still transmitting, whose average number is N_D , and those that come from emitters that are no longer active, but whose emissions still occupy the Galaxy (regardless of whether or not they intersect the Earth). In full generality, $N_G \geq N_D$, where the equality sign holds true either if there are no galactic emissions ($N_G = 0$ and $N_D = 0$) or if the only emissions present in the Galaxy come from emitters currently radiating.

The three quantities N_G , N_D , and \bar{k} are the main statistical parameters characterizing the demography of technosignatures in the Milky Way, from which other quantities and properties of interest can be derived. For example \bar{k}/N_G gives the fraction of galactic emissions intersecting Earth, while it can be demonstrated that $1 - \exp(-\bar{k})$ yields the fraction of the galactic volume occupied by the emissions (Grimaldi 2017). Furthermore, we see from the discussion above that the sequence of nested inequalities,

$$N_G \geq N_D \geq \bar{k}, \quad (2)$$

holds true for all types of EM emissions (isotropic, anisotropic) and for any combination of them, implying that \bar{k} , the quantity that could be possibly estimated from observations, sets a lower limit to the population (N_G) of emissions filling the Galaxy.

Here, we present a detailed study of N_G , N_D , and \bar{k} to ascertain their dependence on the birthrate, the longevity, and the geometry of the emission processes. We base our analysis on the presumption that the rate of technogenesis in the Milky Way has not changed significantly during the

recent history of the Galaxy (a few million years) and that the population of artificial EM sources can be described by a collection of statistically independent emitters.

2 EMISSION PROCESSES

We start by defining our model of emission processes generated by artificial emitters in the Milky Way galaxy. We focus on the thin disk component of the Galaxy containing roughly 10^{10} potentially habitable planets within a radius $R_G \simeq 60$ kly from the galactic centre, located at the origin of a cartesian reference frame with axes x , y , and z . We approximate the thin disk by an effectively two-dimensional disk of radius R_G on the x - y plane. We make the assumption that the artificial emitters are located at random sites $\mathbf{r} = (x, y)$ relative to the galactic centre and that they are statistically independent of each other, meaning that their birthrates and longevities are random variables uncorrelated with \mathbf{r} .

In the following, we shall employ the generic term “emission process” to indicate an artificial EM radiation of any wavelength and power spectrum that is emitted either continuously or not during a time duration L . We shall however distinguish the emission processes according to their isotropy/anisotropy and to the geometry of the volume occupied by their radiations by assigning to them a distinct type or class labelled by the index i . In particular, here we shall focus on three prototypical types of emissions: isotropic radiations ($i = \text{iso}$), randomly directed narrow beams (denoted as “random beams”, $i = \text{rb}$), and narrow beams emitted by rotating lighthouses (denoted simply as “lighthouses”, $i = \text{lh}$). Furthermore, we shall assume that the radiations propagate unperturbed throughout the Galaxy at the speed of light c . In so doing, we are neglecting scattering and absorption processes by the interstellar medium, which is a highly idealized setup meant to illustrate more clearly the effects of the emission geometries.

We allow the possibility that the different types of emission processes can have correspondingly different birthrates and longevities. For example, a continuous isotropic emission in the infrared could be resulting from the waste heat produced by a civilization exploiting the energy of its sun (Dyson 1960), as for type II civilizations of the Kardashev scale (Kardashev 1964). The corresponding emission birthrate would be presumably lower, and the emission longevity longer, than that of a less technologically developed (or less energy harvesting) civilization targeting other planets with radio signals to just advertise its existence. We therefore introduce the rate of appearance per unit area for emitters of type i , $\gamma_i(\mathbf{r}, t)$, defined so that $\gamma_i(\mathbf{r}, t) d\mathbf{r} dt$ gives the expected number of i -emitters within an area element $d\mathbf{r}$ about \mathbf{r} that started emitting within a time interval dt centered at a time t before present. Likewise, we associate to all processes of type i a common probability distribution function (PDF) of the longevity, denoted $\rho_i(L)$, such that $\int_0^\infty dL \rho_i(L) = 1$ for each i .

The emitter rate of emergence vanishes for distances on the galactic disk larger than R_G , so that integrating $\gamma_i(\mathbf{r}, t)$ over \mathbf{r} gives the birthrate of the emission processes of type i in the entire Galaxy:

$$\Gamma_i(t) = \int d\mathbf{r} \gamma_i(\mathbf{r}, t). \quad (3)$$

Table 1. Legend of symbols used in the text and their meaning. The subscript i refers to the different types of emissions considered here: isotropic signals ($i = \text{iso}$), random beams ($i = \text{rb}$), and rotating lighthouses ($i = \text{lh}$).

symbol	meaning
N_D^i	Drake's number of active emitters of type i
\bar{k}_i	average number of i -emissions crossing Earth at the present time
N_G^i	average number of i -emission intersecting the galactic plane
Γ_i	birthrate of emissions of type i
\bar{L}_i	mean longevity of emissions of type i
R_G	radius of the galactic plane (~ 60 kly)
$t_G = 2R_G/c$	travel time of a photon between two opposite edges of the galaxy ($\sim 10^5$ yr)
α_0	angular aperture of a conical beam signal

Finally, owing to the statistical independence of the emission processes, the sum of the birthrates of each type of emission gives the total rate of appearance of all emission processes:

$$\Gamma(t) = \sum_i \Gamma_i(t). \quad (4)$$

2.1 Average number of active emitters (Drake's N_D)

The Drake equation can be directly derived from considering the number of emitters that are currently transmitting (Grimaldi et al. 2018). To see this, we note that for any galactic emitter that started an emission process at a time t in the past, the necessary condition that at present time the emitter is still active is that the time elapsed since its birth is shorter than the emission longevity, that is, $t \leq L$. The time integral of $\Gamma_i(t)$ from $t = 0$ to $t = L$ gives therefore the expected number of emitters of type i and longevity L that are still emitting. The average number of active i -emitters is obtained by marginalizing L with respect to the PDF associated to the processes of type i :

$$N_D^i = \int_0^\infty dL \rho_i(L) \int_0^L dt \Gamma_i(t). \quad (5)$$

We take the time-scale over which the rate $\Gamma_i(t)$ is expected to show appreciable variations to be much larger than L , even for longevity values distributed over several million years. In so doing, we are assuming that the emitter birthrates did not change significantly during the recent history of the Galaxy and can be taken constant in Eq. (5), leading to:

$$N_D^i = \Gamma_i \bar{L}_i, \quad (6)$$

where $\bar{L}_i = \int_0^\infty dL \rho_i(L) L$ is the mean longevity of the emission processes of type i (see Table 1 for a list of symbols used in this paper and their meaning). Equation (6) is the Drake equation relative to signals of type i under the steady-state hypothesis. By setting $x_i = \Gamma_i/\Gamma$ with $\sum_i x_i = 1$, and defining

$$\bar{L} = \sum_i x_i \bar{L}_i \quad (7)$$

as the longevity averaged over all types of emission processes, the sum of N_D^i over all i 's leads to the usual Drake equation in the compact form:

$$N_D = \Gamma \bar{L}. \quad (8)$$

It is worth stressing that the steady-state hypothesis upon which the derivation of Eq. (8) rests would be less justifiable

if we were considering active emitters from a region extending over Giga light-years, as in this case the temporal dependence of the emission birthrates should be taken into account.

2.2 Average number of emission processes at Earth (\bar{k})

While in deriving N_D we only needed to count the number of active emitters without specifying the characteristics of their emission processes, to calculate the mean number of emission processes intersecting Earth, \bar{k} , we have to specify the conditions under which such intersections occur. First, we note that for an emission process that started at a time t in the past, the emitted EM radiations, traveling through space at the speed of light c , fill at the present time a more or less extended region of space that depends on the longevity and directionality of the emission process. This region can be continuous, as in the case of an emission process (either isotropic or anisotropic) lasting a time L without interruptions, or discontinuous as for an emitter having sent during L a sequence of intermittent signals. In the latter case, if we assume that the train of signals is crossing Earth, there is a finite probability of the Earth not being illuminated at a given instant of time (Gray 2020), which may lead us to overlook this process in the calculation of \bar{k} .

Similar considerations apply also to intrinsically continuous emission processes that appear discontinuous or intermittent from the Earth's viewpoint, as it is the case of a rotating beacon whose beamed signal crosses Earth periodically. Also, the signal intermittency may be due to variations in the emitted power with minimum flux at the receiver below the detection threshold (Gray 2020) or to scintillation effects due to the interstellar medium (Cordes et al. 1997).

To avoid ambiguities in determining \bar{k} , we shall treat any intermittent (as seen from the Earth) emission of total longevity L as an effectively continuous process lasting the same amount of duration time. Operatively, we could think of a periodic signal of period T and duty cycle w impinging upon the Earth during an observational time interval Δt . The condition $\Delta t/T \geq 1 - w$ ensures that the "on" phase of the emission crosses Earth at least once during Δt , so that the process is "detectable" with probability one and can be added to the list of processes crossing Earth. We further note that among the requisites an intermittent signal should have to be recognized as a *bona fide* technosignature, the recurrence of detection is one of the most important (Forgan et al. 2019).

2.2.1 Isotropic emissions

Let us consider an emitter located at \mathbf{r} that started emitting an isotropic process at a time t in the past and for a duration L . If the process is intrinsically continuous, at the present time the region of space filled by the EM waves is a spherical concentric shell of outer radius ct and thickness cL , centered on the emitter position \mathbf{r} . In the case of a intermittent isotropic process of period T and duty cycle w , this region encompasses a sequence of nested concentric spherical shells, each of thickness cwT , of consecutive outer radii differing by cT . Conforming to the above prescription for intermittent emissions, we ignore the internal structure of the encompassing shell by treating it as an effectively continuous spherical shell of width cL .

The condition that the shell intersects the Earth is fulfilled by the requirement (Grimaldi 2017; Balbi 2018)

$$ct - cL \leq |\mathbf{r} - \mathbf{r}_E| \leq ct, \quad (9)$$

where \mathbf{r}_E is the vector position of the Earth. If $\gamma_{\text{iso}}(\mathbf{r}, t)$ (where the subscript ‘‘iso’’ stands for isotropic) is the process birthrate per unit volume and $\rho_{\text{iso}}(L)$ is the PDF of the longevity, the average number of spherical shells at Earth is obtained by marginalizing the condition (9) over \mathbf{r} , L , and t :

$$\bar{k}_{\text{iso}} = \int dL \rho_{\text{iso}}(L) \int d\mathbf{r} \int_{|\mathbf{r}-\mathbf{r}_E|/c}^{|\mathbf{r}-\mathbf{r}_E|/c+L} dt \gamma_{\text{iso}}(\mathbf{r}, t). \quad (10)$$

As done in Sec. 2.1, we neglect the temporal dependence of the birthrate, $\gamma_{\text{iso}}(\mathbf{r}, t) \simeq \gamma_{\text{iso}}(\mathbf{r})$, so that Eq. (10) reduces to:

$$\bar{k}_{\text{iso}} = \int dL \rho_{\text{iso}}(L) L \int d\mathbf{r} \gamma_{\text{iso}}(\mathbf{r}) = \Gamma_{\text{iso}} \bar{L}_{\text{iso}}, \quad (11)$$

which, as anticipated in Sec. 2.1, coincides with the Drake number N_D^{iso} relative to isotropic emission processes. Note that since we have taken a time independent birthrate, \mathbf{r}_E has dropped off Eq. (11), meaning that \bar{k}_{iso} actually gives the mean number of emissions crossing any given point in the Galaxy. This holds true also for other types of emission processes as long as the corresponding birthrates do not depend on t .

2.2.2 Anisotropic emissions: random beams and lighthouses

In the case of anisotropic signals, the region of space filled by the EM radiation does not cover all directions and, therefore, only the fraction of signals that are directed towards the Earth can contribute to \bar{k} . For example, a prototypical anisotropic signal often discussed in the literature is that of a conical beam of opening angle α_0 pointing to a given direction over the full lifetime of the emission process. As shown in Appendix A0.1, if such beamed signals are generated with a constant birthrate and their orientation is distributed uniformly over the unit sphere (3D case), the average number of random beams (rb) intersecting Earth will be proportional to the solid angle subtended by the beams, that is:

$$\bar{k}_{\text{rb}} = \frac{\langle \alpha_0^2 \rangle}{16} \Gamma_{\text{rb}} \bar{L}_{\text{rb}}, \quad (3\text{D random beams}) \quad (12)$$

where $\langle \dots \rangle$ denotes an average over the beam apertures (assumed to be narrow), \bar{L}_{rb} is the average longevity of the

beams, and Γ_{rb} is their birthrate. We see therefore that contrary to the case of isotropic emission processes, the mean number of beams crossing Earth can be many orders of magnitude smaller than the corresponding Drake’s number $N_D^{\text{rb}} = \Gamma_{\text{rb}} \bar{L}_{\text{rb}}$. Taking for example beam apertures comparable to that of the Arecibo radar ($\sim 2' \simeq 6 \times 10^{-4}$ rad) Eq. 12 yields $\bar{k}_{\text{rb}}/N_D^{\text{rb}} \sim 2 \times 10^{-8}$, and even smaller values of $\bar{k}_{\text{rb}}/N_D^{\text{rb}}$ are obtained by assuming optical or infrared laser emissions of apertures under an arcsecond (Howard et al. 2004; Tellis & Marcy 2017).

Instead of pointing towards random directions in space, another hypothetical scenario is that in which the emitters generate beams directed preferably along the galactic plane in order to enhance the probability of being detected by other civilizations. In this two dimensional (2D) case, the mean number of beams illuminating the Earth becomes (see A0.1):

$$\bar{k}_{\text{rb}} = \frac{\langle \alpha_0 \rangle}{2\pi} \Gamma_{\text{rb}} \bar{L}_{\text{rb}}, \quad (2\text{D random beams}) \quad (13)$$

so that $\bar{k}_{\text{rb}}/N_D^{\text{rb}} \sim 10^{-4}$ for $\langle \alpha_0 \rangle$ comparable to that of the Arecibo radar.

Another type of anisotropic signal is that of a narrow beam emitted by a rotating source, like a lighthouse rotating with constant angular velocity. This kind of process generates a continuous, radiation-filled spiralling beam revolving around the emitter and expanding at the speed of light. The spiral cross section increases with the beam aperture α_0 and the distance from the source. Even if this kind of process is intrinsically continuous, an expanding spiral impinging upon Earth will be perceived as a periodic sequence of signals. For example, if the spin axis is perpendicular to the galactic plane, the spiral generated by a rotating conical beam of angle aperture α_0 will periodically cross Earth’s line-of-sight with duty cycle $\alpha_0/2\pi$.

In a manner similar to what we have done for the case of intrinsically discontinuous signals, we discard the signal intermittency perceived at Earth by introducing an effective volume encompassing the spiralling beam, whose construction is detailed in the Appendix A0.2. As long as the rotation axes are oriented uniformly over the unit sphere (3D case), we find that the mean number of lighthouse (lh) signals crossing Earth reduces to:

$$\bar{k}_{\text{lh}} = \frac{\langle \alpha_0 \rangle}{2} \Gamma_{\text{lh}} \bar{L}_{\text{lh}}, \quad (3\text{D lighthouses}) \quad (14)$$

while when the spin axes are perpendicular to the galactic plane (2D case), \bar{k}_{lh} becomes:

$$\bar{k}_{\text{lh}} = \Gamma_{\text{lh}} \bar{L}_{\text{lh}}, \quad (2\text{D lighthouses}). \quad (15)$$

The signals generated by lighthouses have therefore much larger values of \bar{k} than those of random beams with comparable birthrates and longevities, as shown in Fig. 1. In particular, from Eqs. (12)-(15) we see that $\bar{k}_{\text{rb}}/\bar{k}_{\text{lh}}$ scales as $\sim \langle \alpha_0 \rangle N_D^{\text{rb}}/N_D^{\text{lh}}$ for 2D or 3D anisotropic signals of similar apertures, meaning for example that over $\sim 10^3$ active Arecibo-like beams must thus be added to each active lighthouse of comparable $\langle \alpha_0 \rangle$ to have analogous values of \bar{k} . Furthermore, \bar{k}_{lh} for the 2D case turns out to be independent of α_0 , as for isotropic processes. This is an interesting result, implying that an observer on Earth has the same chances of being illuminated by a 2D lighthouse as by a (pulsed) isotropic signal if the two have equal Drake’s numbers, Fig. 1.

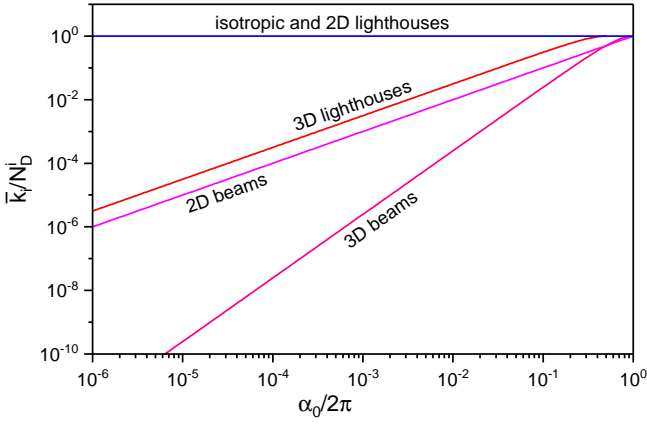


Figure 1. Average number of emissions of type i crossing Earth, \bar{k}_i , over the corresponding Drake number N_D^i plotted as a function of the beam aperture α_0 for the different types i of processes considered in this work.

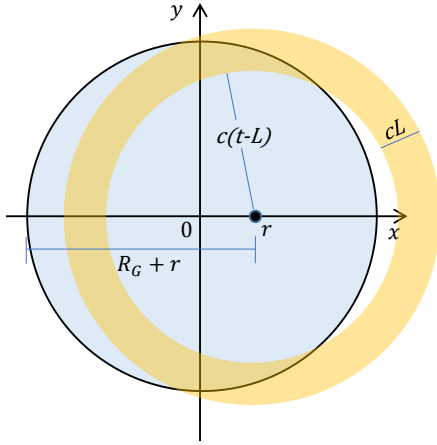


Figure 2. Top view of the galactic disk of radius R_G with superimposed areas covered by emissions of different geometries originated by a source located at $(r, 0)$. (a): the intersection with the plane x - y of the spherical shell generated by an isotropic emission forms an annulus of inner radius $c(t-L)$, which intersects the galactic disk if $c(t-L) \leq R_G + r$.

2.3 Average number of emission processes intersecting the Galaxy (N_G)

So far, the only temporal variable required to calculating N_D^i and \bar{k}_i has been the signal longevity L . In deriving N_G , we shall introduce an additional time-scale,

$$t_G = \frac{2R_G}{c}, \quad (16)$$

defined as the time required by a photon to travel, unperturbed, across two opposite edges of the Milky Way ($\approx 10^5$ yr). Contrary to L and Γ_i , t_G is an astrophysical quantity, specific to our Galaxy, that is independent of any assumption about the existence and/or the properties of the artificial emissions.

2.3.1 Isotropic emissions

The necessary condition for an isotropic signal intersecting the Galaxy is that there is a non-null intersection between the spherical shell and the galactic disk. As shown in Fig. 2, this is fulfilled by requiring the inner radius of the shell to be smaller than the maximum distance of the emitter from the edge of the galactic disk, that is, $c(t-L) \leq r + R_G$. The number of isotropic emissions intersecting the Galaxy is therefore:

$$\begin{aligned} N_G^{\text{iso}} &= \int dL \rho_{\text{iso}}(L) \int d\mathbf{r} \int_0^{(r+R_G)/c+L} dt \gamma_{\text{iso}}(\mathbf{r}) \\ &= \Gamma_{\text{iso}} \bar{L}_{\text{iso}} + \frac{1}{c} \int d\mathbf{r} \gamma_{\text{iso}}(\mathbf{r}) (r + R_G). \end{aligned} \quad (17)$$

Using a birthrate that is uniform over the entire galactic disk, $\gamma_{\text{iso}}(\mathbf{r}) = \theta(R_G - r) \Gamma_{\text{iso}} / \pi R_G^2$, the above expression reduces to:

$$N_G^{\text{iso}} = \Gamma_{\text{iso}} \left(\bar{L}_{\text{iso}} + \frac{5}{6} t_G \right), \quad (18)$$

where t_G is the time-scale given in Eq. (16). Other functional forms of $\gamma_{\text{iso}}(\mathbf{r})$ affects only the prefactor of t_G . For example, taking $\gamma_{\text{iso}}(\mathbf{r}) \propto \theta(R_G - r) \exp(-r/r_s)$ with $r_s = 8.15$ kly (Grimaldi & Marcy 2018), the numerical factor $5/6$ (≈ 0.833) in (18) becomes ≈ 0.646 .

An interesting feature of Eq. (18) is that using (11) we can replace Γ_{iso} by $\bar{k}_{\text{iso}} / \bar{L}_{\text{iso}}$, yielding:

$$N_G^{\text{iso}} = \bar{k}_{\text{iso}} \left(1 + \frac{5}{6} \frac{t_G}{\bar{L}_{\text{iso}}} \right), \quad (19)$$

so that for $\bar{L}_{\text{iso}} \ll t_G \approx 10^5$ yr the expected number of the emissions intersecting the Galaxy can be much larger than that of the emissions crossing Earth. For example, even if \bar{k}_{iso} is only ≈ 0.1 and $\bar{L}_{\text{iso}} \approx 10^2$ yr, N_G^{iso} is nevertheless of the order 10^2 . As we shall see below, the directionality of the signals can amplify even more the difference between \bar{k}_i and N_G^i .

2.3.2 Anisotropic emissions: random beams and lighthouses

The calculations of the average number of random beams present in the Galaxy, N_G^{rb} , and the one relative to the lighthouse signals, N_G^{lh} , are detailed in the Appendixes A0.3 and A0.4, respectively. Here we report only the final expressions obtained under the assumption of small opening angles and a spatially uniform birthrate of the emitters:

$$N_G^{\text{rb}} = \begin{cases} \Gamma_{\text{rb}} \left(\bar{L}_{\text{rb}} + \frac{\langle \alpha_0 \rangle}{2} \frac{4}{3\pi} t_G \right), & \text{3D random beams} \\ \Gamma_{\text{rb}} \left(\bar{L}_{\text{rb}} + \frac{4}{3\pi} t_G \right), & \text{2D random beams,} \end{cases} \quad (20)$$

$$N_G^{\text{lh}} = \begin{cases} \Gamma_{\text{lh}} \left(\bar{L}_{\text{lh}} + \frac{2}{\pi} t_G \right), & \text{3D lighthouses} \\ \Gamma_{\text{lh}} \left(\bar{L}_{\text{lh}} + \frac{5}{6} t_G \right), & \text{2D lighthouses.} \end{cases} \quad (21)$$

The relevant result of these calculations is that for all but one case (that is, the 3D random beams) the mean number of anisotropic emissions intersecting the galactic plane is

Table 2. Analytic expressions of the average number of emissions intersecting the Galaxy, N_G , and the expected number of processes at Earth, \bar{k} , for the different types of emissions considered in this article. Γ_i is the birthrate of emissions of type i (with $i = \text{iso}$ for isotropic signals, $i = \text{rb}$ for random beams, and $i = \text{lh}$ for rotating lighthouses) and \bar{L}_i is the corresponding mean longevity. α_0 denotes the beam aperture. For all cases, the corresponding Drake's number is $N_D^i = \Gamma_i \bar{L}_i$.

type	N_G	\bar{k}
isotropic	$\Gamma_{\text{iso}} (\bar{L}_{\text{iso}} + \frac{5}{6} t_G)$	$\Gamma_{\text{iso}} \bar{L}_{\text{iso}}$
3D random beams	$\Gamma_{\text{rb}} (\bar{L}_{\text{rb}} + \frac{\langle \alpha_0 \rangle}{2} \frac{4}{3\pi} t_G)$	$\frac{\langle \alpha_0^2 \rangle}{16} \Gamma_{\text{rb}} \bar{L}_{\text{rb}}$
2D random beams	$\Gamma_{\text{rb}} (\bar{L}_{\text{rb}} + \frac{4}{3\pi} t_G)$	$\frac{\langle \alpha_0 \rangle}{2\pi} \Gamma_{\text{rb}} \bar{L}_{\text{rb}}$
3D lighthouses	$\Gamma_{\text{lh}} (\bar{L}_{\text{lh}} + \frac{2}{\pi} t_G)$	$\frac{\langle \alpha_0 \rangle}{2} \Gamma_{\text{lh}} \bar{L}_{\text{lh}}$
2D lighthouses	$\Gamma_{\text{lh}} (\bar{L}_{\text{lh}} + \frac{5}{6} t_G)$	$\Gamma_{\text{lh}} \bar{L}_{\text{lh}}$

independent of the angular aperture, and is therefore comparable to that obtained for the case of isotropic emissions with similar birthrates and longevitys.

3 DISCUSSION

Table 2 summarizes the analytic expressions of N_G^i and \bar{k}_i derived in the previous section. For each type of emission process, the Drake number $N_D^i = \Gamma_i \bar{L}_i$ is the only quantity that does not depend on the geometry of the emission process and we shall therefore focus our discussion primarily on \bar{k}_i and N_G^i .

Figures 3-5 show \bar{k}_i as a function of the mean signal longevity \bar{L}_i and the population of signals in the Galaxy N_G^i , with $i = \text{iso}$ (isotropic, Fig. 3), $i = \text{rb}$ (random beams, Fig. 4), and $i = \text{lh}$ (lighthouses, Fig. 5). The results have been obtained by taking $R_G = 60$ kly for the galactic radius, corresponding to $t_G = 2R_G/c = 1.2 \times 10^5$ yr. The red solid lines demarcate the boundary between $\bar{k}_i > 1$ (red colour scale) and $\bar{k}_i < 1$ (blue colour scale), while the black solid lines indicate N_G^i calculated for constant values of the emission birthrate Γ_i . The results shown in Figs. 4 and 5 have been obtained assuming $\langle \alpha_0^2 \rangle \simeq \langle \alpha_0 \rangle^2$ and an average beam aperture of $2'$, corresponding to $\langle \alpha_0 \rangle \simeq 6 \times 10^{-4}$ rad. Results for different beam apertures can be easily obtained using the expressions in Table 2.

A first interesting feature is the behaviour of the galactic population of technosignatures, N_G^i , as a function of \bar{L}_i for fixed Γ_i (black solid lines). While N_G^i increases proportionally to the signal longevity for $\bar{L}_i \gtrsim t_G$, reaching asymptotically the corresponding Drake's number $N_D^i = \bar{L}_i \Gamma_i$, for $\bar{L}_i \lesssim t_G \sim 10^5$ yr it reduces to

$$N_G^i \simeq \Gamma_i t_G \simeq \Gamma_i \times (10^5 \text{ yr}), \quad (22)$$

for all types of emission processes with the exception of random beams in 3D. In this case N_G^{rb} scales as $\langle \alpha_0 \rangle \Gamma_{\text{rb}} t_G$ for $\bar{L}_{\text{rb}} \lesssim \langle \alpha_0 \rangle t_G$.

Equation (22) is remarkable because it prescribes the galactic population of emission processes to be proportional to only the birthrate Γ_i , regardless of the signal longevity as long as it is assumed \bar{L}_i to be less than $\sim 10^5$ yr. This is an advantage compared to the Drake's number N_D^i , where in addition

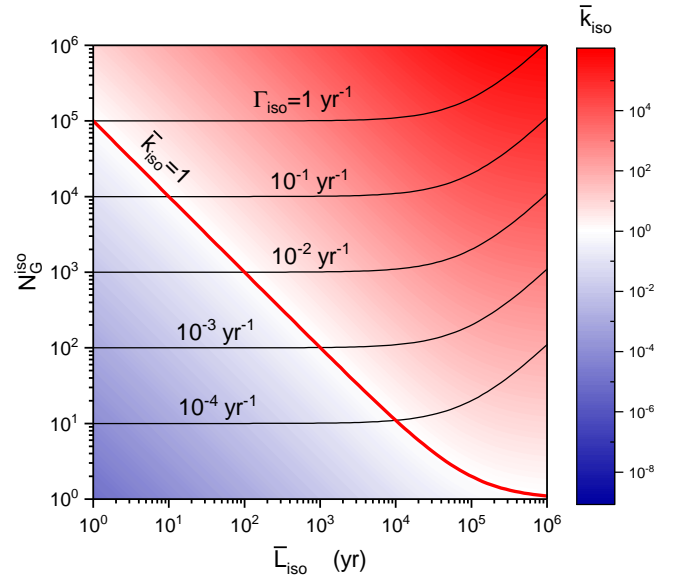


Figure 3. Expected number of isotropic emission processes at Earth, \bar{k}_{iso} , as a function of the mean signal longevity \bar{L}_{iso} and the average number N_G^{iso} of isotropic emissions intersecting the Galaxy. The red solid line indicates the special value $\bar{k}_{\text{iso}} = 1$, while the black solid lines show N_G^{iso} calculated for different values of the emission birthrate Γ_{iso} .

to Γ_i the longevity of the signals is a further object of speculations. For a wide range of \bar{L}_i values, we can thus conjecture about the size of N_G^i by reasoning only in terms of the signal birthrate. To this end it is instructive to compare Γ_i with the rate of formation of habitable planets in the Milky Way, Γ_P , whose estimates place it in the range 0.01-0.1 planet per year (Behroozi & Peebles 2015; Zackrisson et al. 2016; Gobat & Hong 2016; Anchordoqui et al. 2018).

Let us first make the hypothesis that each habitable planet can be the potential source of no more than one artificial emission. This would correspond to Γ_P being a theoretical upper limit of Γ_i . Under this assumption, the resulting galactic population of both isotropic emissions (Fig. 3) and rotating beacons (Fig. 5) would be bounded from above by $\max(N_G^i) \sim 10^3$ - 10^4 , or somewhat less for 2D random beams of Fig. 4(a), which is essentially the number of habitable planets being formed during a timespan of order $t_G \sim 10^5$ yr.

Such an upper limit of N_G entails a corresponding lower bound on the average distance a_E between the emitters. Indeed, since within our working assumption N_G corresponds to the number of emitters releasing the emissions, their number density can be expressed as $\rho_E = N_G/\pi R_G^2$. This allows us to find from $\pi a_E^2 \rho_E \sim 1$ that $a_E \sim R_G/\sqrt{N_G}$, thereby implying that the lower bound on a_E is of the order 10^3 ly for $\bar{L} \lesssim t_G$. Following the same reasoning, we see that the typical relative distance between emitters estimated by the Drake equation, $a_D \sim R_G/\sqrt{N_D}$, scales for $\bar{L} \lesssim t_G$ as $a_D \sim a_E \sqrt{t_G/\bar{L}}$. The difference between a_G and a_D stems from the fact that the Drake's number gives the average population of active emitters, which are only a fraction of all N_G emitters whose signals are present in the Galaxy. For example, while assuming $\Gamma_i \sim \Gamma_P$ and $\bar{L} \lesssim 10$ yr gives $N_G \sim 10^3$ and $a_E \sim 10^3$ ly, the Drake equation yields $N_D \lesssim 1$ and a value of a_D comparable

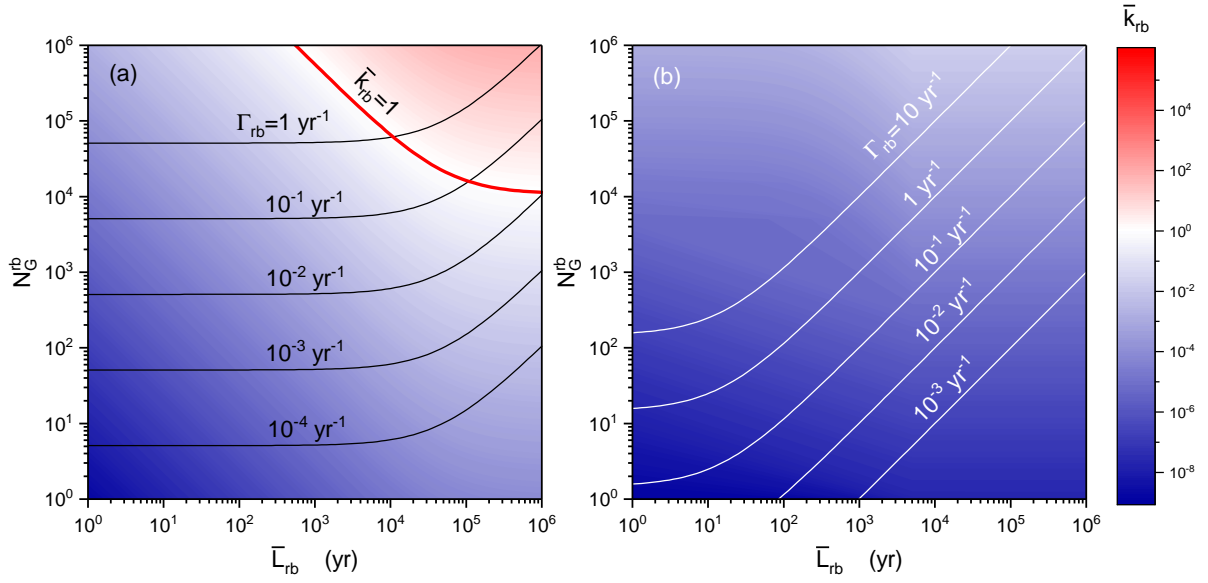


Figure 4. Expected number of random narrow beams crossing Earth, \bar{k}_{rb} , as a function of their mean longevity \bar{L}_{rb} and the average number N_G^{rb} of beams intersecting the Galaxy. In panel (a) the orientations of the beam axes are distributed uniformly along the galactic disk (2D case), while in panel (b) they are distributed uniformly over the 3D space. The beam aperture is fixed at $2'$, corresponding to $\alpha_0 = 6 \times 10^{-4}$ rad. The red solid lines indicate the special value $\bar{k}_{rb} = 1$, while the black solid lines show N_G^{rb} calculated for different values of the emission birthrate Γ_{rb} .

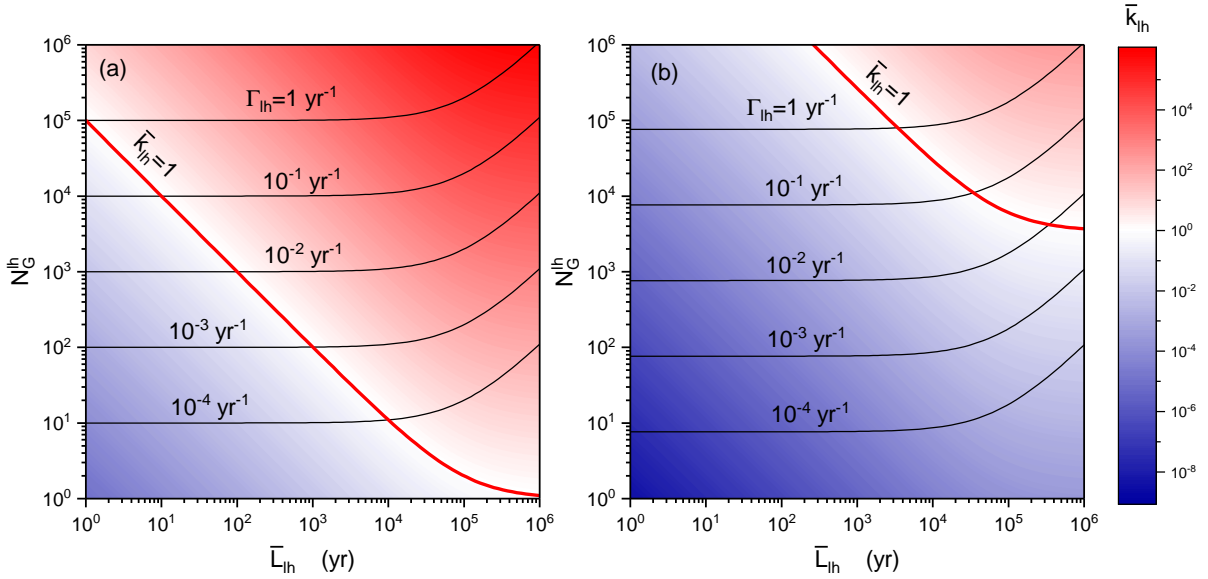


Figure 5. Expected number of emissions from rotating beacons crossing Earth, \bar{k}_{lh} , as a function of their mean longevity \bar{L}_{lh} and the average galactic population N_G^{lh} . In panel (a) the orientations of the spin axes are kept perpendicular to the galactic plane (2D case), while in panel (b) they are distributed uniformly over the 3D space. The red solid lines indicate the special value $\bar{k}_{lh} = 1$, while the black solid lines show N_G^{lh} calculated for different values of the emission birthrate Γ_{lh} .

to or larger than the diameter of the Galaxy, meaning that in this case out of $\sim 10^3$ galactic emissions essentially none comes from currently active emitters.

As we have seen in the previous section, in addition to N_D the longevity \bar{L} constraints also the number of the emission processes crossing our planet, which is further affected by the directionality of the signals (Fig. 2). Assuming therefore a large number of galactic emissions does not automatically

imply similarly large values of \bar{k}_i . For example, even taking $\Gamma_i \sim 0.1 \text{ yr}^{-1}$ (that is, $N_G^i \simeq 10^4$ for $\bar{L}_i < t_G$), the expected maximum value of \bar{k}_i ranges from $\sim 10^3$ for $\bar{L}_i = 10^4$ yr down to ~ 0.1 for $\bar{L}_i = 1$ yr in the case of isotropic emissions (Fig. 3) and 2D lighthouses [Fig. 5(a)]. Within the same range of signal longevitys, the upper bound on \bar{k}_i of beams in 2D and rotating beacons in 3D drops to only $\sim 10^{-5}$ - 10^{-1} , Figs. 4(a) and 5(b).

A special situation is represented by a collection of beamed signals with axis orientations distributed in the 3D space [Fig. 4(b)]. In this case, N_G^{rb} becomes independent of the signal longevity only when $\bar{L}_{\text{rb}} \lesssim \langle \alpha_0 \rangle t_G$, which for $\langle \alpha_0 \rangle \sim 2'$ represents lifetimes smaller than ~ 10 yr. In this limit, $N_G^{\text{rb}} \lesssim 1$ for $\Gamma_{\text{rb}} \sim 0.1 \text{ yr}^{-1}$ and the resulting \bar{k}_{rb} is upper bounded by a negligible $\sim 5 \times 10^{-8}$. Values of N_G of the order of 10^5 can nevertheless be reached for 3D beams lasting at least 1 Myr, but even in this case \bar{k}_{rb} is only $\sim 2 \times 10^{-3}$.

Let us pause one moment to consider the implications of assuming each habitable planet being the potential source of at most one emission process. As shown above, this hypothesis entails an upper bound of N_G^i of the order 10^3 - 10^4 , implying therefore the possibility of technogenesis arising on *each* habitable planet during the last $\sim 10^5$ years. This exceeds by far the most optimistic stances, as such an assumption would imply not only a non-zero probability that abiogenesis is ubiquitous in the Milky Way, but also that intelligence and technology are inevitable outcomes of the evolutionary path of life on each inhabited planet. As long as a one-to-one correspondence between emission processes and planets is maintained, an upper bound on Γ_i (and so on N_G^i) should be more reasonably placed to much lower values than Γ_P , leading to $\max(N_G^i) \ll 10^3$ - 10^4 and to correspondingly small values of \bar{k}_i .

Our model, however, does not distinguish whether the emission events have occurred once or multiple times within t_G on a given planet, nor does it rule out the possibility of the emitters far outnumbering the planets in which technology arose, as for example self-replicating robotized lighthouses swarming in the free space. Within such scenarios, Γ_i could thus be larger than the rate of emergence of technological civilizations capable of releasing technosignatures and perhaps even comparable to, or in excess of, Γ_P . The plausibility of a galactic population of $\sim 10^4$ short lived (i.e., $\bar{L}_i \lesssim t_G$) emissions should however be weighed against the requirement that all these emissions must have been released during the last $\sim 10^5$ years in order to fill the galaxy.

Of course, it is still possible to have significantly large values of N_G^i and \bar{k}_i even for relatively low birthrates if the mean longevity is so long to prevail over the small values of Γ_i . For example, signals emitted from isotropic sources or 2D lighthouses with a rate as small as $\sim 10^{-5} \text{ yr}^{-1}$ would bring values of N_G^i and \bar{k} larger ~ 100 if their longevities exceeded ~ 10 Myr. Similar values of N_G^i are obtained for 2D beams and 3D lighthouses with $\Gamma_i \sim 10^{-5} \text{ yr}^{-1}$ and $\bar{L}_i \sim 10$ Myr, but the reduced solid angle for $\langle \alpha_0 \rangle \sim 2'$ makes \bar{k}_i as small as $\sim 10^{-2}$ (which drops to $\sim 10^{-8}$ in the case of 3D random beams).

So far, we have discussed each type of emission processes separately to study the effect of Γ_i , \bar{L}_i and of the signal directionality on N_G^i and \bar{k}_i . However, in the most general case, different types of processes may be present simultaneously in the Galaxy and the contribution of each i -process to the total N_G and \bar{k} depends on the respective occurrence frequency. To see this, we note that the different expressions of N_G^i and \bar{k}_i given in Table 2 have the form $N_G^i = \Gamma_i(\bar{L}_i + u_i t_G)$ and $\bar{k}_i = v_i \Gamma_i \bar{L}_i$, where u_i and v_i are the dimensionless factors taking account the geometry and the directionality of the signals. Owing to the assumed statistical independence of the emitters, the quantities N_D , N_G , and \bar{k} are simple linear combinations of the different types of processes. We can

thus write:

$$N_G = \sum_i \Gamma_i(\bar{L}_i + u_i t_G) = \Gamma \bar{L} + \Gamma t_G \sum_i x_i u_i, \quad (23)$$

$$\bar{k} = \sum_i v_i \Gamma_i \bar{L}_i = \Gamma \sum_i x_i v_i \bar{L}_i, \quad (24)$$

where, as done in Sec.2.1, $x_i = \Gamma_i/\Gamma$ and $\bar{L} = \sum_i x_i \bar{L}_i$. Considerations similar to those discussed in the previous section apply therefore also to the more general case. In particular, as seen from Eq. (23), as long as the total signal longevity \bar{L} is smaller than $\sim t_G \sim 10^5$ yr, the total number of processes intersecting the Galaxy results to be proportional to $\Gamma t_G \sim (10^5 \text{ yr}) \times \Gamma$, regardless of \bar{L} . Speculations about the abundance of short-lived ($\bar{L} \lesssim 10^5$ yr) emissions in the Galaxy can thus be framed in terms of possible upper bounds on the total birthrate Γ .

From Eq. (24) we see that the contribution of each type of emission to the total number of processes crossing Earth strongly depends on the relative abundance of signal types and their longevities. As shown in Figs. 3-5, the contribution to \bar{k} of isotropic processes and lighthouses in 2D would likely dominate over other types of emissions of similar birthrates. For example, assuming that the fraction of rotating beacons sweeping the galactic plane is comparable to that of 3D beamed emissions, $x_{\text{lh}} \sim x_{\text{rb}}$, the two would contribute equally to \bar{k} only if the mean longevity of the 3D beams is about $16/\langle \alpha_0^2 \rangle$ times larger than that of the rotating beacons. For beam apertures of $2'$ this corresponds to a factor $\sim 10^7$, so for a given fraction of 2D lighthouses lasting in average 10 years an equal amount of 3D beams requires a longevity of ~ 100 Myr to contribute equally to \bar{k} .

As a last consideration, we note that the total birthrate Γ in Eqs. (23) and (24) can be eliminated using the Drake number $N_D = \Gamma \bar{L}$, yielding:

$$N_G = N_D \left(1 + \frac{t_G}{\bar{L}} \sum_i x_i u_i \right), \quad (25)$$

$$\bar{k} = N_D \sum_i x_i v_i \frac{\bar{L}_i}{\bar{L}}, \quad (26)$$

allowing us to translate in terms of N_G and \bar{k} the rich literature devoted to the Drake equation. By further eliminating N_D from (25) and (26) we get

$$\frac{\bar{k}}{N_G} = \frac{\sum_i x_i v_i \bar{L}_i}{\bar{L} + t_G \sum_i x_i u_i}, \quad (27)$$

which expresses the fraction of galactic signals crossing Earth in terms of the remaining unknown temporal variables: the longevities. We note that Eq. 27 generalizes a similar formula derived for the case of isotropic signals in Grimaldi et al. (2018) and Grimaldi & Marcy (2018). The two formulas are however not fully equivalent because in those works \bar{k} was put in relation to the number of emission processes released during the last t_G years rather than using the number N_G of emissions physically intersecting the Galaxy.

4 CONCLUSIONS

In this paper, we have introduced other statistical quantities than the Drake number N_D to characterize the population of EM technosignatures in the Milky Way. We have considered

the average number of EM emissions present in the Galaxy, N_G , and the average number \bar{k} of emissions intersecting the Earth (or any other site in the Galaxy). Unlike N_D , \bar{k} and N_G provide measures of the number of emission processes that are not necessarily released by currently active emitters, but that can be potentially detected on Earth (\bar{k}) or that still occupy physically the Galaxy (N_G). In order to study how these indicators are affected by the signal directionality we have considered in addition to the case of isotropic emission processes also strongly anisotropic ones like narrow beams pointing in random directions and rotating beacons.

Under the assumption that the emission birthrates did not change during the recent history of the Galaxy, we have shown that $\bar{k} = N_D$ only for isotropic processes and for emissions originating from rotating beacons sweeping the galactic disk. In all the other cases considered (beamed signals directed randomly and lighthouses with tilted rotation axis) \bar{k} can be orders of magnitudes smaller than the Drake number, showing that N_D may largely overestimate the possible occurrence of signals that can be remotely detected.

We have further discussed at length N_G as the proper indicator of the galactic abundance of technosignatures. We have shown that N_G , leaving aside the special case of narrow beams directed uniformly in 3D space, is only marginally affected by the signal directionality. A central result of the present study is that N_G becomes independent of the signal longevity if this is shorter than about 10^5 ly, yielding therefore a measure of the abundance of galactic technosignatures that depends only on the emission birthrate.

ACKNOWLEDGEMENTS

The author thanks Amedeo Balbi and Geoffrey W. Marcy for fruitful discussions.

DATA AVAILABILITY

The data underlying this article are available in the article.

REFERENCES

- Anchordoqui, L. A., Weber, L. A., Soriano, J. F., 2017, Proc. 35th International Cosmic Ray Conference PoS(ICRC2017). International School for Advanced Studies, Trieste, Italy, p. 254
- Balbi, A. 2018, *Astrobiology* 18, 54
- Behroozi, P., Peebles, M. S., 2015, *MNRAS*, 454, 1811
- Ćirković, M. M., 2004, *Astrobiology*, 4, 225.
- Cordes, J. M., Lazio, J. W., Sagan, C., 1997, *ApJ*, 487, 782
- Drake, F. D., 1961, *Physics Today*, 14, 40.
- Drake, F. D., 1965, *The radio search for intelligent extraterrestrial life*. In *Current Aspects of Exobiology*, Pergamon Press, New York, p. 323
- Dressing, C. D., & Charbonneau, D. 2013, *ApJ*, 767, 95
- Dyson, F. J., 1960, *Science*, 131, 1667.
- Enriquez, J. E., Siemion, A., Foster, G., et al. 2017, *ApJ*, 849, 104
- Flodin, M., 2019, *Determining upper limits on galactic ETI civilizations transmitting continuous beacon signals in the radio spectrum* (Dissertation). Retrieved from <http://urn.kb.se/resolve?urn=urn:nbn:se:kth:diva-266824>
- Forgan, D., H., 2009, *Int. J. Astrobiol.*, 8, 121.
- Forgan, D. 2014, *JBIS*, 67, 232

- Forgan, D. et al., 2019, *Int. J. Astrobiol.*, 18, 336
- Frank, A., Sullivan III, W. T., 2016, *Astrobiology*, 16, 359.
- Glade, N., Ballet, P., Bastien, O., 2016, *Int. J. Astrobiol.*, 11, 103.
- Gobat, R., Hong, S. E., 2016, *Å*, 592, A96
- Gray, R. H. 2020, *Int. J. astrobiol.* 1-9; doi.org/10.1017/S1473550420000038
- Grimaldi, C. 2017, *Sci. Rep.*, 7, 46273
- Grimaldi, C., Marcy, G. W., Tellis, N. K., Drake, F., 2018, *PASP*, 130, 054101.
- Grimaldi, C., Marcy, G. W., 2018, *Proc. Natl. Acad. Sci. U.S.A.*, 115, E9755.
- Howard, A. W., Horowitz, P., Wilkinson, D. P., et al. 2004, *ApJ*, 613, 1270
- Isaacson, H., Siemion, A. P. V., Marcy, G. W., Lebofsky, M. et al. 2017, *PASP*, 129, 054501
- Kardashev, N. S., 1964, *Soviet Astronomy*, 8, 217.
- Kiang, N. Y. et al., 2018, *Astrobiology*, 18, 619.
- Maccione, C., 2010, *Acta Astronaut.*, 67, 1366.
- Petigura, E. A., Howard, A. W., & Marcy, G.W. 2013, *Proc. Natl. Acad. Sci. U.S.A.*, 110, 19273
- Prantzos N., 2013, *Int. J. Astrobiol.*, 12, 246.
- Prantzos, N., 2019, *MNRAS*, 493, 3464.
- Price, D., C., et al., 2019, *AJ*, 159, 86.
- Seager, S., 2018, *Int. J. Astrobiol.*, 17, 294.
- Tarter, J. 2001, *Annu. Rev. Astron. Astrophys.* 35, 511.
- Tellis, N. K., Marcy, G. W. 2017, *AJ*, 153, 251
- Wolfe, J. H., Billingham, J., Edelson, R. E., et al. 1981, in *Proc. Life in the Universe*, NASA Conf. Publication 2156, ed. J. Billingham (Cambridge, MA: MIT Press), 391
- Wright, J. T., Kanodia, S., Lubar, E., 2018, *AJ*, 156, 260.
- Zackrisson, E., Calissendorff, P., Gonzalez, J., et al., 2016, *AJ833*, 214.
- Zink, J. K., Hansen, B. M. S., 2019, *MNRAS*, 487, 246.

APPENDIX A: ANISOTROPIC EMISSIONS

A0.1 \bar{k} for random beams

Let us consider an emitter located at \mathbf{r} transmitting since a time t before present a conical beam of aperture α_0 (Forgan 2014; Grimaldi 2017). During the entire lifetime L of the emission, the beam axis is held oriented along the direction of a unit vector \hat{n} . The region of space filled by the radiation is the intersection between a cone of apex at \mathbf{r} and a spherical shell centred on the cone apex with outer radius ct and thickness cL . As done for the isotropic case, we neglect the internal structure of this region arising in the case of an intermittent beam.

The angular sector formed by the overlap of the conical beam with the galactic plane (grey region in Fig. A1) subtends the angle

$$\beta = \begin{cases} 2 \arccos \left[\frac{\cos(\alpha_0/2)}{\sin(\theta)} \right], & |\theta - \pi/2| \leq \alpha_0/2 \\ 0, & \text{otherwise} \end{cases} \quad (\text{A1})$$

where $\theta \in [0, \pi]$ is the angle formed by \hat{n} with the z -axis. From this construction, we see that the beam will cross the Earth if \mathbf{r}_E is located within the angular sector, that is, if Eq. (9) is satisfied and $|\phi| \leq \beta/2$, where ϕ is the angle formed by $\mathbf{r}_E - \mathbf{r}$ and the projection of \hat{n} on the x - y plane, Fig. A1.

By adopting a constant birthrate of beamed signals with random orientations of \hat{n} , the integration over t under the condition (9) yields the factor L , as in Eq. (11). Introducing the random beam (rb) emission rate Γ_{rb} and the corre-

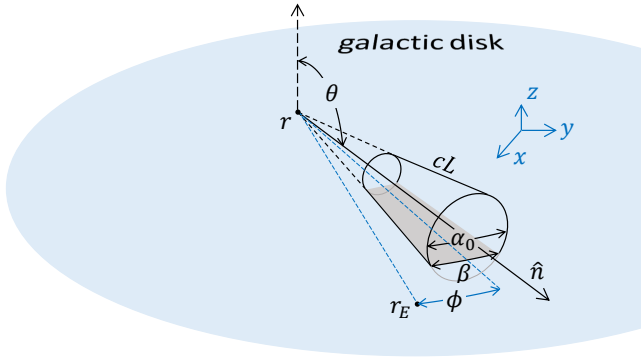


Figure A1. Schematic illustration of a beamed emission of duration L and aperture α_0 . The Earth and the emitter positions are denoted respectively by the vectors \mathbf{r} and \mathbf{r}_E . The beam axis of the lighthouse is oriented along the direction \hat{n} and forms an angle θ with the z -axis. ϕ is the angle formed by the direction of $\mathbf{r} - \mathbf{r}_E$ and the projection of \hat{n} over the galactic disk. The grey region denotes the overlap area between the galactic disk and the beam.

sponding average longevity \bar{L}_{rb} , the mean number of beamed signals crossing Earth reduces therefore to:

$$\bar{k}_{rb}(\alpha_0) = \Gamma_{rb} \bar{L}_{rb} \int d\hat{n} g(\hat{n}) \Theta(\beta/2 - |\phi|), \quad (\text{A2})$$

where $d\hat{n} = d\phi d\theta \sin\theta$, $g(\hat{n})$ is the PDF of the direction of \hat{n} , and $\Theta(x) = 1$ for $x \geq 0$ and $\Theta(x) = 0$ or $x < 0$ is the unit step function.

In the case in which the beams are oriented uniformly in three dimensions (3D), the PDF of \hat{n} is $g(\hat{n}) = 1/4\pi$ and using Eq. (A1) the integration over \hat{n} yields $\frac{1}{2}[1 - \cos(\alpha_0/2)]$, which is simply the fractional solid angle subtended by the beam (Grimaldi 2017). For beam directions distributed uniformly over the two-dimensional (2D) galactic plane, $g(\hat{n})$ is a Dirac-delta function peaked at $\theta = \pi/2$, $g(\hat{n}) = \delta(\theta - \pi/2)/2\pi$, and the orientational average reduces simply to $\alpha_0/(2\pi)$. For random 3D and 2D beam orientations we obtain therefore:

$$\bar{k}_{rb}(\alpha_0) = \begin{cases} \frac{1 - \cos(\alpha_0/2)}{2} \Gamma_{rb} \bar{L}_{rb}, & \text{3D random beams,} \\ \frac{\alpha_0}{2\pi} \Gamma_{rb} \bar{L}_{rb}, & \text{2D random beams.} \end{cases} \quad (\text{A3})$$

Under the assumption that the beams have angular apertures distributed over small values of α_0 , Eq. (A3) reduces to:

$$\bar{k}_{rb} = \langle \bar{k}_{rb}(\alpha_0) \rangle \simeq \begin{cases} \frac{\langle \alpha_0^2 \rangle}{16} \Gamma_{rb} \bar{L}_{rb}, & \text{3D random beams,} \\ \frac{\langle \alpha_0 \rangle}{2\pi} \Gamma_{rb} \bar{L}_{rb}, & \text{2D random beams,} \end{cases} \quad (\text{A4})$$

where $\langle \dots \rangle$ denotes an average over the α_0 values.

A0.2 \bar{k} for lighthouses

We take a lighthouse (lh) located at \mathbf{r} that started transmitting at a time t in the past and for a duration L a conical

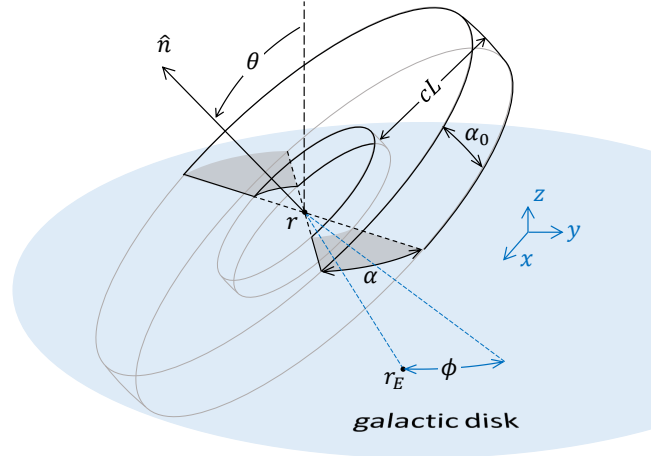


Figure A2. Graphical representation of the effective volume encompassing the regions swept during a time duration L by a lighthouse (or rotating beacon) of beam aperture α_0 . The Earth and the emitter positions are denoted respectively by the vectors \mathbf{r} and \mathbf{r}_E . The spin axis of the lighthouse is oriented along the unit vector \hat{n} and forms an angle θ with the z -axis. The grey region denotes the overlap area between the galactic disk and the effective volume.

beam of angular aperture α_0 . The effective volume encompassing the region physically filled by the EM radiation is formed by the overlap between the volume swept by a cone (of aperture α_0) rotating about the spin axis \hat{n} with apex at \mathbf{r} and a spherical shell concentric to \mathbf{r} of outer radius ct and thickness cL (see Fig. A2). The overlap of the effective volume with the galactic plane forms two annular sectors (shown by grey areas in Fig. A2), symmetric with respect to the line of nodes formed by the intersection of the rotation plane with the galactic disk, and subtending the angle α given by

$$\alpha = \begin{cases} \pi, & 0 \leq \theta \leq \alpha_0/2, \\ 2 \arcsin \left[\frac{\sin(\alpha_0/2)}{\sin(\theta)} \right], & \alpha_0/2 < \theta \leq \pi/2, \end{cases} \quad (\text{A5})$$

where now $\theta \in [0, \pi/2]$ is the angle formed by \hat{n} with the z direction. As done for the case of random beamed signals, the intersection of the angular sector with the Earth is given by the condition (9) and $|\phi| \leq \alpha/2$, where ϕ is the angle formed by $\mathbf{r}_E - \mathbf{r}$ and the line of nodes (see Fig. A2). For a constant birthrate of the lighthouses, the average number of randomly distributed spiralling beams crossing Earth is thus given by:

$$\bar{k}_{lh}(\alpha_0) = \Gamma_{lh} \bar{L}_{lh} \int d\hat{n} g(\hat{n}) \Theta(\alpha/2 - |\phi|), \quad (\text{A6})$$

If \hat{n} is distributed uniformly over the unit sphere (3D case), using Eq. (A5) and $g(\hat{n}) = 1/4\pi$, the integral over θ reduces exactly to $\sin(\alpha_0/2)$ for $\alpha_0 \leq \pi$ and 1 otherwise. In the case the spin axis is perpendicular to the galactic plane (2D case), $g(\theta)$ is a Dirac-delta peak at $\theta = 0$, so that the angular average in Eq. (A6) yields 1. Expanding Eq. (A6) for small beam apertures, $\bar{k}_{lh} = \langle \bar{k}_{lh}(\alpha_0) \rangle$ reads:

$$\bar{k}_{lh} = \begin{cases} \frac{\langle \alpha_0 \rangle}{2} \Gamma_{lh} \bar{L}_{lh}, & \text{3D lighthouses,} \\ \Gamma_{lh} \bar{L}_{lh}, & \text{2D lighthouses.} \end{cases} \quad (\text{A7})$$

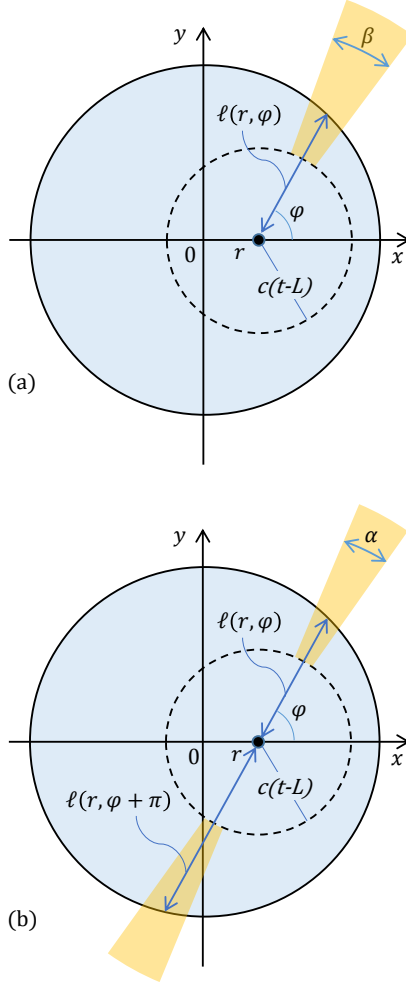


Figure A3. Top view of the galactic disk of radius R_G with superimposed areas covered by emissions of different geometries originated by a source located at $(r, 0)$. (a): The intersection of a beam with the x - y plane forms an annular sector (orange region) subtending an angle β , Eq. (A1), and an inner arc at distance $c(t-L)$ from the emitter. $\ell(r, \varphi)$ is the distance from the emitter to the edge of the Galaxy along the direction of the beam axis projected on the x - y plane. A narrow beam intersects the galactic disk when $c(t-L) \leq \ell(r, \varphi)$. (b): The two annular sectors of angle α , Eq. (A5), denote the overlap area between the x - y plane and the effective volume spanned by a rotating lighthouse with spin axis tilted with respect to the z -axis (see Fig. A2). The intersection of the galactic disk with the rotation plane forms two segments of length $\ell(r, \varphi)$ and $\ell(r, \varphi + \pi)$. The longest of them must be larger than $c(t-L)$ in order for the effective volume to intersect the galactic disk.

A0.3 N_G for random beams

In deriving the average number of random beams intersecting the Galaxy, N_G^{rb} , we shall retain only the contributions at the lowest order in the beam aperture α_0 , which simplifies considerably the calculation. We take an emitter to be located along the x -axis, $\mathbf{r} = (r, 0)$, with the beam axis directed along \hat{n} forming an azimuthal angle φ with \mathbf{r} , Fig. A3(a). The projection of the beam axis on the x - y plane defines the distance

$$\ell(r, \varphi) = \sqrt{R_G^2 - r^2 \sin^2(\varphi)} - r \cos(\varphi) \quad (\text{A8})$$

measured from the emitter position to the edge of the Galaxy (i.e. the circle of radius R_G). As seen from Eq. (A1), the intersection of the beam with the x - y plane is non-null only if the polar angle of \hat{n} is such that $|\theta - \pi/2| \leq \alpha_0/2$. Since $\alpha_0 \ll 1$, \hat{n} lies approximately on the x - y plane and a beam emitted at time t for a duration L will intersect the galactic disk only when $c(t-L)$ is smaller than $\ell(r, \varphi)$, as shown in Fig. A3(a). Conversely, if $|\theta - \pi/2| > \alpha_0/2$ the only beams that intersect the galactic disk are those that are still being transmitted at the present time, that is, those such that $t < L$. After integration over t , N_G^{rb} at the lowest order in α_0 is therefore given by:

$$\begin{aligned} N_G^{\text{rb}} &= \int dL \rho_{\text{rb}}(L) \int d\mathbf{r} \gamma_{\text{rb}}(\mathbf{r}) \int d\hat{n} g(\hat{n}) \\ &\times \left[L + \Theta\left(\frac{\alpha_0}{2} - \left|\theta - \frac{\pi}{2}\right|\right) \frac{\ell(r, \varphi)}{c} \right] \\ &= \Gamma_{\text{rb}} \bar{L}_{\text{rb}} + t_G \frac{\eta}{\pi} \int d\mathbf{r} \gamma_{\text{rb}}(\mathbf{r}) E(r/R_G), \end{aligned} \quad (\text{A9})$$

where $\eta = \alpha_0/2$ or $\eta = 1$ if the direction of \hat{n} is distributed uniformly in 3D space or in the x - y plane, and $E(x) = \int_0^{\pi/2} d\varphi \sqrt{1 - x^2 \sin^2(\varphi)}$ is the complete elliptic integral of the second kind. Using a birthrate that is constant over the galactic disk, the integration over \mathbf{r} yields:

$$N_G^{\text{rb}} = \begin{cases} \Gamma_{\text{rb}} \left(\bar{L}_{\text{rb}} + \frac{\langle \alpha_0 \rangle}{2} \frac{4}{3\pi} t_G \right), & \text{3D random beams} \\ \Gamma_{\text{rb}} \left(\bar{L}_{\text{rb}} + \frac{4}{3\pi} t_G \right), & \text{2D random beams,} \end{cases} \quad (\text{A10})$$

from which we see that N_G^{rb} of narrow beams depends on the angular aperture only in the 3D case.

A0.4 N_G for lighthouses

In the case the spin axis of a rotating beacon is parallel to the z -axis, the effective volume encompassing the radiation (Fig. A2) intersects the Galaxy as long as $c(t-L)$ is smaller than the maximum distance of the emitter from the galactic edge, in full equivalence with the isotropic case. Assuming a spatially uniform birthrate, the number of rotating beacon signals intersecting the Milky Way is thus $N_G^{\text{lh}} = \Gamma_{\text{lh}} (\bar{L}_{\text{lh}} + \frac{5}{6} t_G)$, as in Eq. (18).

In the more general case in which \hat{n} forms an angle θ with the z -direction, at the lowest order in α_0 it suffices to calculate N_G^{lh} by considering the intersection of the rotation plane with the galactic disk, which forms an angle φ with the x -axis. As shown in Fig. A3(b), the emitter, located at $(r, 0)$, cuts the intersection line in two segments, generally of different lengths. The longest of these segments has length $\ell_{\text{max}}(r, \varphi) = \ell(r, \varphi + \pi)$ for $0 \leq \varphi \leq \pi/2$ and $\ell_{\text{max}}(r, \varphi) = \ell(r, \varphi)$ for $\pi/2 \leq \varphi \leq \pi$, where $\ell(r, \varphi)$ is given in Eq. (A8). Since a non-null intersection with the galactic disk is obtained by requiring the inner edge of the effective volume, $c(t-L)$, to be smaller than $\ell_{\text{max}}(r, \varphi)$, we obtain:

$$\begin{aligned} N_G^{\text{lh}} &= \int dL \rho_{\text{lh}}(L) \int d\mathbf{r} \gamma_{\text{lh}}(\mathbf{r}) \int d\hat{n} g(\hat{n}) \left[L + \frac{\ell_{\text{max}}(r, \varphi)}{c} \right] \\ &= \Gamma_{\text{lh}} \bar{L}_{\text{lh}} + \frac{t_G}{\pi} \int d\mathbf{r} \gamma_{\text{lh}}(\mathbf{r}) [E(r/R_G) + r/R_G], \end{aligned} \quad (\text{A11})$$

where we have assumed that the orientation of \hat{n} is distributed uniformly over 3D. For a spatially uniform $\gamma_{\text{lh}}(\mathbf{r})$ the integration over \mathbf{r} yields $2\Gamma_{\text{lh}}$, so that for the two cases examined (\hat{n} random and $\hat{n} \parallel z$) N_G^{lh} reduces to:

$$N_G^{\text{lh}} = \begin{cases} \Gamma_{\text{lh}} \left(\bar{L}_{\text{lh}} + \frac{2}{\pi} t_G \right), & \text{3D lighthouses} \\ \Gamma_{\text{lh}} \left(\bar{L}_{\text{lh}} + \frac{5}{6} t_G \right), & \text{2D lighthouses.} \end{cases} \quad (\text{A12})$$

This paper has been typeset from a $\text{\TeX}/\text{\LaTeX}$ file prepared by the author.